Reaction of $(\mu\text{-H})Os_3(CO)_{10}(\mu_3\text{-CPh})$ with diphenylacetylene. Alkylidyne–alkyne coupling and the crystal structure of $Os_3(CO)_8(\mu,\eta^2\text{-CPhCHPh})(\mu,\eta^3\text{-C}_3Ph_3)$

Melvyn Rowen Churchill *, Joseph W. Ziller

Department of Chemistry, University at Buffalo,
State University of New York, Buffalo, New York 14214 (U.S.A.)

John R. Shapley * and Wen-Yann Yeh

Department of Chemistry, University of Illinois, Urbana, Illinois 61801 (U.S.A.)

(Received March 17th, 1988)

Abstract

The reaction of diphenylacetylene with $(\mu\text{-H})Os_3(CO)_{10}(\mu_3\text{-CPh})$ yields two isomers (**A** and **B**) of stoichiometry $Os_3(CO)_8(H(CPh)_5)$ and two isomers (**C** and **D**) of stoichiometry $Os_3(CO)_9(H(CPh)_5)$. The interconversions of these species have been studied and an X-ray structural study of **B** shows it to be $Os_3(CO)_8(\mu,\eta^2\text{-CPhCHPh})(\mu\text{-}\eta^3\text{-C}_3Ph_3)$ containing a σ,π-vinyl and a dimetalla–allyl fragment. Compound **B** crystallizes in the centrosymmetric monoclinic space group $P2_1/c$ (No. 14) with a 10.1908(18), b 16.6521(23), c 23.1817(48) Å, β 91.725(16)°, V 3932.1(12) Å^3 and $Z = 4$.

Introduction

We have previously reported the synthesis and crystal structure of $(\mu\text{-H})Os_3(CO)_{10}(\mu_3\text{-CPh})$ [1]. The thermal reactivity of $(\mu\text{-H})Os_3(CO)_{10}(\mu_3\text{-CPh})$ is determined by CO dissociation to generate a coordinatively unsaturated species, presumably $[HOs_3(CO)_9(\mu_3\text{-CPh})]$, which then can undergo oxidative addition either intramolecularly with a phenyl C–H bond to give an orthometallated product $(\mu\text{-H})Os_3(CO)_9(\mu_3,\eta^3\text{-CHC}_6H_4)$ or intermolecularly with H_2 to give $(\mu\text{-H})_3Os_3(CO)_9(\mu_3\text{-CPh})$ [1]. The latter result suggests that the intermediate might also react with unsaturated hydrocarbons. Described in this paper are results concerning the reaction of $(\mu\text{-H})Os_3(CO)_{10}(\mu_3\text{-CPh})$ with diphenylacetylene together with the X-ray crystal structure of one of the products.

Experimental

(μ-H)Os$_3$(CO)$_{10}$(μ$_3$-CPh) was prepared by the method previously described [1]. Diphenylacetylene (Aldrich) was used directly as received. N-heptane was distilled from sodium before use. Preparative thin-layer chromatographic (TLC) plates were prepared from Silica Gel GF (Type 60, E. Merck). Melting points were determined in sealed capillaries. ^{1}H and ^{13}C NMR spectra were obtained on a Nicolet NT-360 spectrometer at 360 MHz and 90.56 MHz, respectively. IR spectra were taken on a Perkin–Elmer 281 B spectrometer and were calibrated with polystyrene film and cyclohexane (2138.5 cm^{-1}). Elemental analyses were performed by the Microanalytical Laboratory of the School of Chemical Sciences at the University of Illinois. Field desorption mass spectra were obtained by the staff of the Mass Spectroscopy Laboratory of the School of Chemical Sciences on a Varian-MAT 731 mass spectrometer.

Reaction of (μ-H)Os$_3$(CO)$_{10}$(μ$_3$-CPh) with diphenylacetylene

(μ-H)Os$_3$(CO)$_{10}$(μ$_3$-CPh) (103 mg, 0.11 mmol), diphenylacetylene (43 mg, 0.24 mmol) and n-heptane (25 ml) were placed in a 100 ml round-bottomed flask, equipped with a reflux condenser and a magnetic stir bar. The solution was refluxed under nitrogen for 4.5 h, at which point the color was purple. The solvent was removed under vacuum and the residue subjected to TLC, eluting with n-pentane/dichloromethane (4/1 v/v). A small amount of (μ-H)Os$_3$(CO)$_{10}$(μ$_3$-CPh) (5 mg, 5%) was recovered from the first band. Crystallization of the second, yellow band from dichloromethane/methanol gave air-stable, yellow crystals of (μ-H)Os$_3$(CO)$_9$(μ$_3$,η^3-(CPh)$_3$) (17 mg, 0.015 mmol, 14%). Crystallization of the third, orange-red band from n-pentane produced air-stable, *red* crystals characterized as Os$_3$(CO)$_8$(H(CPh)$_5$) (**A**) (16 mg, 0.013 mmol, 12%). Crystallization of the fourth, purple band from n-hexane yielded air-stable, *purple* needle crystals of Os$_3$(CO)$_8$(H(CPh)$_5$) (**B**) (36 mg, 0.029 mmol, 26%). Isolation of the material forming the fifth, yellow band produced a *yellow* solid of Os$_3$(CO)$_9$(H(CPh)$_5$) (**C**) (13 mg, 0.01 mmol, 9%). Crystallization of the last, orange-yellow band from dichloromethane/methanol produced *orange-yellow* crystals of Os$_3$(CO)$_9$(H(CPh)$_5$) (**D**) (23 mg, 0.018 mmol, 17%).

(μ-H)Os$_3$(CO)$_9$(μ$_3$,η^3-(CPh)$_3$). M.p. 195–197°C. Anal. Found: C, 32.90; H, 1.71. Os$_3$C$_{30}$H$_{16}$O$_9$ calc: C, 33.03; H, 1.48%. Mass spectrum: *m/z* 1096 (*M*$^+$, ^{192}Os). IR (C$_6$H$_{12}$): ν(CO) 2097s, 2073vs, 2046vs, 2019s, 2013s, 2003s, 1997w, 1991ms, 1982m cm^{-1}. ^{1}H NMR (CDCl$_3$, 17°C): δ 7.10–6.66 (m, 15H), −18.16 (s, 1H). ^{13}C NMR (CDCl$_3$, 17°C): δ 177.5 (s, 2*C*O), 174.6 (s, 2*C*O), 174.2 (s, 3*C*O), 171.1 (d, 2*C*O, ^2J(C–H) 11 Hz), 162.4 (br, *C*-Ph).

Os$_3$(CO)$_8$(H(CPh)$_5$ (A). Mass spectrum: *m/z* 1246 (*M*$^+$, ^{192}Os). IR (C$_6$H$_{12}$): ν(CO) 2080m, 2052s, 2013vs, 2003s, 1991m, 1977w, 1960 cm^{-1}. ^{1}H NMR (CDCl$_3$, 17°C): δ 7.31–6.19 (m 25H, Ph), 5.11 (s, 1H, CH). ^{13}C NMR (CDCl$_3$, −55°C): δ 186.8 (s, 1*C*O); 180.7 (s, 1*C*O), 179.6 (s, 1*C*O), 176.3 (s, 1*C*O), 175.8 (s, 1*C*O), 175.6 (s, 1*C*O), 174.9 (s, 1*C*O), 174.1 (s, 1*C*O), 155.2 (s, 0.5C, *C*-Ph), 130.5 (s, 0.5C, *C*-Ph).

Os$_3$(CO)$_8$(H(CPh)$_3$) (B). Anal. Found: C, 41.36; H, 2.33. Os$_3$C$_{43}$H$_{26}$O$_8$ calc: C, 41.61; H, 2.11%. Mass spectrum: *m/z* 1246 (*M*$^+$, ^{192}Os). IR (C$_6$H$_{12}$): ν(CO) 2084s, 2049vs, 2023vs, 2013s, 2003w, 1986m, br, 1971 m br, 1959 m, br cm^{-1}. ^{1}H NMR ((CD$_3$)$_2$CO, 17°C): δ 7.56–6.67 (m, Ph), 6.29 (s, 1H, CH). ^{13}C NMR (CDCl$_3$,

$-55°C$): δ 187.0 (s, 1CO), 183.1 (s, 1CO), 182.2 (s, 1CO), 181.6 (s, 1CO). 176.8 (s, 1CO), 175.8 (s, 1CO), 174.9 (s, 1CO), 172.7 (s, 1CO), 121.4 (s, 0.5C, C-Ph), 109.8 (s, 0.5C, C-Ph).

$Os_3(CO)_9(H(CPh)_5)$ (C). Mass spectrum: m/z 1274 (M^+, ^{192}Os). IR (C_6H_{12}): ν(CO) 2092s, 2074s, 2023s, 2009s, 2003s, 1965vw, br, 1923w, br cm^{-1}. ^1H NMR (CDCl$_3$, 17°C): δ 7.32–6.64 (m, 25H, Ph), 5.05 (s, 1H, CH). ^{13}C NMR (CDCl$_3$, $-55°C$): δ 218.8 (s, 1CO), 187.4 (s, 1CO), 183.4 (s, 1CO), 179.5 (s, 1CO), 174.1 (s, 1CO), 173.1 (s, 1CO), 172.7 (s, 1CO), 172.2 (s, 1CO), 171.6 (s, 1CO), 148.8 (s, CPh).

$Os_3(CO)_9(H(CPh)_5)$ (D). Anal. Found: C, 41.34; H, 2.04. $Os_3C_{44}H_{26}O_9$ calc: C, 41.64; H, 2.06%. Mass spectrum: m/z 1274 (M^+, ^{192}Os). IR (C_6H_{12}): ν(CO) 2088m, 2072vs, 2068sh, 2030m, 2022vs, 2004s, 1998s, 1992sh, 1966m, br cm^{-1}. ^1H NMR (CDCl$_3$, 17°C): δ 7.57–6.74 (m, 25H, Ph), 4.42 (s, 1H, CH). ^{13}C NMR (CDCl$_3$, $-55°C$): 203.3 (s, 0.5CO; d, 0.25CO, ^2J(C–C) 18 Hz; d, 0.25CO, ^2J(C–C) 35 Hz), 183.0 (s, 0.5CO; d, 0.5CO, ^2J(C–C) 18 Hz), 178.4 (s, 1CO), 176.7 (br, 1CO), 174.5 (s, 1CO), 173.7 (br, 1CO), 172.8 (s, 1CO), 171.7 (br, 1CO), 170.5 (s, 1CO), 129.2 (s, 0.5C, CPh), 90.0 (s, 0.25C; d, 0.25C, ^2J(C–C) 35 Hz; CPh).

The crystals of $Os_3(CO)_8(H(CPh)_5)$ (B) found suitable for X-ray analysis were grown from dichloromethane/methanol at 25°C.

Attempted reaction of $(\mu$-H)Os$_3(CO)_9(\mu_3,\eta^3$-(CPh)$_3)$ with diphenylacetylene

A solution of $(\mu$-H)Os$_3(CO)_9(\mu_3,\eta^3$-(CPh)$_3)$ (11 mg, 0.01 mmol) and diphenyl-acetylene (9 mg, 0.05 mmol) in n-heptane (5 ml) was added into an oven-dried, 25 ml round-bottomed flask equipped with a reflux condenser and a magnetic stir bar. The solution was refluxed under nitrogen for 5 h, but no reaction occurred.

Attempts to interconvert $Os_3(CO)_8(H(CPh)_5)$ (A) and $Os_3(CO)_8(H(CPh)_5)$ (B)

A solution of $Os_3(CO)_8(H(CPh)_5)$ (B) (purple isomer, 6 mg, 5 μmol) in n-heptane (5 ml) was refluxed under nitrogen for 3 h, but no evidence for the presence of the red isomer A was observed. Similarly, heating a solution of $Os_3(CO)_8(H(CPh)_5)$ (A) (red isomer) did not generate the B isomer.

Reaction of $Os_3(CO)_8(H(CPh)_5)$ (B) with carbon monoxide

An oven-dried 50 ml three-necked round-bottom flask was equipped with a magnetic stir bar. One neck was stoppered, one was fitted with a reflux condenser connected to an oil bubbler, and the third neck had an inlet tube for introduction of gas into the solution. A solution of $Os_3(CO)_8(H(CPh)_5)$ (B) (13 mg, 0.01 mmol) in n-heptane (15 ml) was transferred to the flask. With carbon monoxide bubbling through the solution, it was refluxed for 3.5 h. The solvent was removed under vacuum and the residue subjected to TLC, eluting with n-pentane/dichloromethane (4/1, v/v). $Os_3(CO)_8(H(CPh)_5)$ (A) (1 mg, 8%), $Os_3(CO)_8(H(CPh)_5)$ (B) (4 mg, 31%), $Os_3(CO)_9(H(CPh)_5)$ (C) (6 mg, 45%), and $Os_3(CO)_9(H(CPh)_5)$ (D) (1 mg, 7%) were obtained.

Reaction of $Os_3(CO)_8(H(CPh)_5)$ (A) with carbon monoxide

$Os_3(CO)_8(H(CPh)_5)$ (A) (7 mg, 5.6 μmol) was treated with carbon monoxide by the procedure described above and afforded $Os_3(CO)_8(H(CPh)_5)$ (A) (4 mg, 57%), $Os_3(CO)_8(H(CPh)_5)$ (B) (trace amount), $Os_3(CO)_9(H(CPh)_5)$ (C) (ca. 0.5 mg), and $Os_3(CO)_9(H(CPh)_5)$ (D) (2 mg, 28%).

Thermolysis of Os₃(CO)₉(H(CPh)₅) (D).

An oven-dried 25 ml round-bottomed flask was equipped with a reflux condenser and a magnetic stir bar. To the flask was added a solution of $Os_3(CO)_9(H(CPh)_5)$ (**D**) (14 mg, 0.011 mmol) in n-heptane (10 ml) which was refluxed under nitrogen for 4 h. The solvent was removed under vacuum and the residue subjected to TLC, eluting with n-pentane/dichloromethane (4/1, v/v). $(\mu\text{-H})Os_3(CO)_9(\mu_3,\eta^3\text{-}(CPh)_3)$ (< 1 mg), $Os_3(CO)_8(H(CPh)_5)$ (**A**) (3 mg, 22%), $Os_3(CO)_8(H(CPh)_5)$ (**B**) (6 mg, 44%) and $Os_3(CO)_9(CPh)_5)$ (**D**) (2 mg, 14%) were obtained but no $Os_3(CO)_9(H(CPh)_5)$ (**C**) was produced.

Thermolysis of Os₃(CO)₉(H(CPh)₅) (C)

$Os_3(CO)_9(H(CPh)_5)$ (**C**) (8 mg, 6.3 μmol) in n-heptane was thermolyzed and worked up by the procedure described above, affording $(\mu\text{-H})Os_3(CO)_9(\mu_3\text{-}\eta^3\text{-}(CPh)_3)$ (trace amount), $Os_3(CO)_8(H(CPh)_5)$ (**A**) (1 mg, 13%), $Os_3(CO)_8(H(CPh)_5)$ (**B**) (3 mg, 38%) and $Os_3(CO)_9(H(CPh)_5)$ (**C**) (2 mg, 25%). No evidence for the formation of $Os_3(CO)_9(H(CPh)_5)$ (**D**) was observed.

Collection of X-ray diffraction data on Os₃(CO)₈(H(CPh)₅) (isomer B)

A very limited quantity of this material was available. Following unsuccessful efforts to 'trim' one large crystal, we elected to use the remaining rather plate-like crystal in its available form. This had approximate dimensions $0.05 \times 0.25 \times 0.50$ mm and was mounted in a thin-walled glass capillary and aligned on the Syntex P2₁ automated four-circle diffractometer at SUNY-Buffalo. Laue symmetry determination, crystal class, unit cell parameters and the crystal's orientation matrix were

Table 1

Experimental data for the X-ray diffraction study of $Os_3(CO)_8(\mu,\eta^2\text{-CPhCHPh})(\mu,\eta^3\text{-}C_3Ph_3)$ (**B**)

Formula: $C_{43}H_{26}O_8Os_3$

Fw: 1241.3

Crystal system: monoclinic

Space group: $P2_1/c$ (C_{2h}^5; No. 14)

a 10.1908(18) Å

b 16.6521(23) Å

c 23.1817(48) Å

β 91.725(16)°

V 3932.1(12) Å³

$Z = 4$

D_{calc} (g/cm³) = 2.10

Diffractometer: Syntex P2₁

Radiation: Mo-K_α ($\bar{\lambda}$ 0.710730 Å)

Monochromator: Highly oriented graphite

Scan type: Coupled θ (crystal)–2θ(counter)

Scan width: Symmetrical $[2\theta(K_{\alpha_1}) - 0.9] \to [2\theta(K_{\alpha_2}) + 0.9]$

Scan speed: 4.0° min⁻¹ (in 2θ)

2θ range (°): 4.5–40.0

μ(Mo-K_α) (cm⁻¹) = 103.0

Absorption correction: Empirical (ψ-scan method)

Data collected: $+ h$, $+ k$, $\pm l$ (Total 3957)

Unique reflections: 3687

Table 2

Final positional and thermal parameters for $Os_3(CO)_8(\mu,\eta^2\text{-CPhCHPh})(\mu,\eta^3\text{-}C_3Ph_3)$ (**B**)

Atom	x	y	z	$B_{(iso)}$ ($\mathring{A}^2$)
Os(1)	0.36676(12)	0.09456(8)	0.36174(7)	
Os(2)	0.09996(12)	0.07281(8)	0.34299(7)	
Os(3)	0.22491(13)	0.13826(8)	0.45277(7)	
O(11)	0.6369(21)	0.1238(13)	0.3305(11)	3.79(51)
O(12)	0.4951(24)	−0.0324(16)	0.4387(12)	5.30(62)
O(21)	−0.0237(28)	−0.0615(18)	0.4086(14)	6.91(74)
O(22)	−0.0568(27)	0.0288(17)	0.2342(14)	6.37(70)
O(23)	−0.0970(22)	0.2060(14)	0.3726(11)	4.15(54)
O(31)	0.3586(26)	0.1949(16)	0.5640(13)	5.82(66)
O(32)	−0.0113(28)	0.2059(17)	0.5030(14)	6.53(71)
O(33)	0.2070(24)	−0.0300(16)	0.5024(12)	5.18(61)
C(11)	0.5140(31)	0.1066(19)	0.3416(16)	3.24(74)
C(12)	0.4468(35)	0.0174(23)	0.4110(18)	4.32(86)
C(21)	0.0242(28)	−0.0057(18)	0.3881(15)	2.30(65)
C(22)	0.0052(35)	0.0493(21)	0.2756(18)	4.13(85)
C(23)	−0.0212(36)	0.1524(23)	0.3671(18)	4.61(89)
C(31)	0.3091(31)	0.1746(18)	0.5187(16)	2.84(71)
C(32)	0.0851(37)	0.1701(22)	0.4796(18)	4.74(91)
C(33)	0.2119(33)	0.0342(22)	0.4844(17)	3.86(81)
C(4)	0.2593(29)	0.0065(18)	0.3071(15)	2.89(71)
C(41)	0.2713(32)	−0.0839(20)	0.3011(17)	3.54(77)
C(42)	0.2737(31)	−0.1186(20)	0.2462(16)	3.36(76)
C(43)	0.2736(36)	−0.2011(23)	0.2392(19)	4.76(90)
C(44)	0.2834(36)	−0.2480(22)	0.2898(19)	4.60(89)
C(45)	0.2879(32)	−0.2179(20)	0.3456(16)	3.32(75)
C(46)	0.2851(35)	−0.1349(23)	0.3499(18)	4.56(87)
C(5)	0.3035(28)	0.0674(17)	0.2696(14)	2.29(65)
C(51)	0.3953(30)	0.0606(18)	0.2223(15)	2.66(69)
C(52)	0.3615(33)	0.0971(20)	0.1681(17)	3.73(78)
C(53)	0.4529(39)	0.0929(24)	0.1203(19)	5.3(10)
C(54)	0.5635(41)	0.0531(25)	0.1266(21)	5.8(10)
C(55)	0.5983(39)	0.0146(25)	0.1767(20)	5.6(10)
C(56)	0.5073(31)	0.0161(19)	0.2256(16)	3.19(74)
C(6)	0.2280(28)	0.1369(17)	0.2892(14)	2.25(64)
C(61)	0.2459(32)	0.2186(19)	0.2623(16)	3.45(77)
C(62)	0.1194(32)	0.2536(20)	0.2450(16)	3.47(76)
C(63)	0.1177(33)	0.3283(20)	0.2124(17)	3.73(79)
C(64)	0.2357(32)	0.3613(20)	0.1985(16)	3.55(77)
C(65)	0.3548(33)	0.3278(21)	0.2150(17)	3.94(82)
C(66)	0.3603(34)	0.2573(21)	0.2464(17)	3.97(81)
C(7)	0.3625(28)	0.2139(17)	0.4007(14)	2.35(66)
C(71)	0.4842(33)	0.2556(21)	0.4153(17)	3.82(80)
C(72)	0.5107(34)	0.3282(21)	0.3954(17)	4.04(82)
C(73)	0.6335(42)	0.3637(26)	0.4119(21)	6.1(11)
C(74)	0.7117(41)	0.3309(25)	0.4500(21)	5.6(10)
C(75)	0.6825(44)	0.2583(28)	0.4785(22)	6.9(12)
C(76)	0.5684(31)	0.2170(19)	0.4599(16)	3.06(73)
C(8)	0.2426(26)	0.2520(16)	0.3991(14)	1.74(60)
C(81)	0.2013(30)	0.3351(18)	0.4230(15)	2.68(69)
C(82)	0.1116(33)	0.3804(21)	0.3855(16)	3.69(79)
C(83)	0.0762(44)	0.4547(28)	0.4064(23)	6.9(12)
C(84)	0.1274(40)	0.4899(25)	0.4542(21)	5.7(10)
C(85)	0.2283(38)	0.4471(23)	0.4830(19)	5.04(94)
C(86)	0.2659(30)	0.3695(19)	0.4672(15)	2.85(70)

Table 2 (continued)

Anisotropic temperature factors ($\mathring{A}^2$) [a]

Atom	B_{11}	B_{22}	B_{33}	B_{12}	B_{13}	B_{23}
Os(1)	2.016(64)	2.371(66)	2.671(81)	0.077(49)	−0.660(53)	0.075(58)
Os(2)	2.194(67)	2.942(69)	3.009(86)	−0.313(50)	−0.666(57)	−0.019(60)
Os(3)	2.556(67)	3.108(73)	2.394(81)	0.184(52)	−0.550(52)	0.026(59)

[a] The anisotropic thermal parameters enter the expression for the calculated structure factor in the form:
$\exp[-0.25(h^2 a^{*2} B_{11} + k^2 b^{*2} B_{22} + l^2 c^{*2} B_{33} + 2hka^* b^* B_{12} + 2hla^* c^* B_{13} + 2klb^* c^* B_{23})]$.

carried out by previously described techniques [2]. Room temperature (22°C) intensity data were collected using the θ–2θ scan technique with Mo-K_α radiation under the conditions given in Table 1. All 3957 data were corrected for the effects of absorption and for Lorentz and polarization effects and were placed on an approximately absolute scale by means of a Wilson plot. It should be noted that diffraction data were rather weak; an accurate structural study was not anticipated. A careful survey of a preliminary data set revealed the systematic extinctions $0k0$ for $k = 2n + 1$ and $h0l$ for $l = 2n + 1$; the diffraction symmetry was $2/m$. The centrosymmetric monoclinic space group $P2_1/c$ (C_{2h}^5; No. 14) is thus uniquely defined [3].

Solution and refinement of the crystal structure

All crystallographic calculations were carried out using our locally modified version of the Syntex XTL crystallographic computing package. The analytical scattering factors for neutral atoms were used throughout the analysis [4a]; both the real ($\Delta f'$) and imaginary ($i\,\Delta f''$) components of anomalous dispersion [4b] were included. The function minimized during full-matrix least squares refinement was $\sum w(|F_o| - |F_c|)^2$ where $1/w = [\sigma(|F_o|)]^2 + [0.015|F_o|]^2$.

The structure was solved by direct methods using MULTAN [5]; the positions of the three osmium atoms were located from an "E-map". Subsequent difference-Fourier syntheses revealed the positions of all remaining non-hydrogen atoms. Hydrogen atom contributions were included in calculated idealized positions with d(C–H) 0.95 Å [6]. Refinement of positional and thermal parameters (anisotropic for the osmium atoms) led to convergence with $R_F = 9.9\%$, $R_{wF} = 9.3\%$ and $GOF = 2.73$ for 232 variables refined against all 3687 unique data, ($R_F = 7.4\%$, $R_{wF} = 9.0\%$ for those 2735 data with $|F_o| > 6\sigma(|F_o|)$). The largest peak in the final difference-Fourier map was of height 2.2 e $\mathring{A}^{-3}$ and close to the position of Os(2).

Final parameters are collected in Table 2.

Results and discussion

Reaction of (μ-H)Os$_3$(CO)$_{10}$(μ-CPh) with diphenylacetylene

Treatment of (μ-H)Os$_3$(CO)$_{10}$(μ_3-CPh) with diphenylacetylene in refluxing n-heptane solution generates (μ-H)Os$_3$(CO)$_9$(μ_3,η^3-(CPh)$_3$), Os$_3$(CO)$_8$(H(CPh)$_5$) (A and B isomers), and Os$_3$(CO)$_9$(H(CPh)$_5$) (C and D isomers). The transformations of these products are shown in Scheme 1.

There are two separable isomers for each of Os$_3$(CO)$_9$(H(CPh)$_5$) (C and D) and Os$_3$(CO)$_8$(H(CPh)$_5$) (A and B). The C and D isomers of Os$_3$(CO)$_9$(H(CPh)$_5$) are
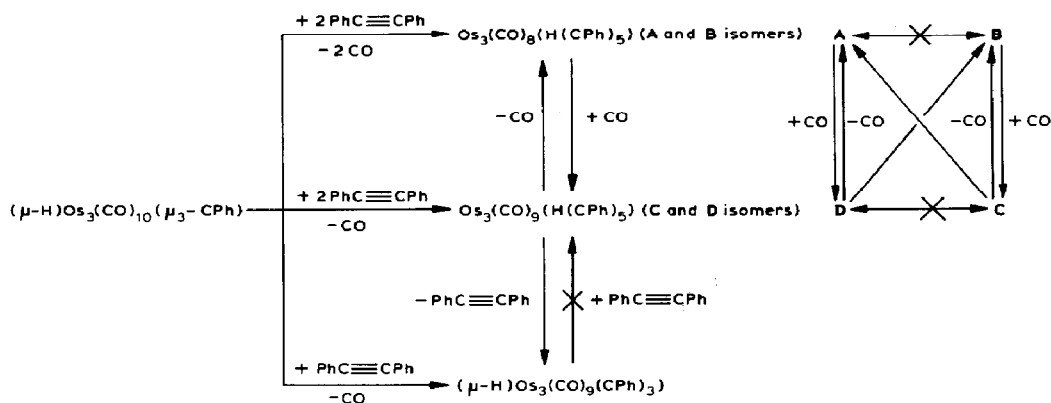
Scheme 1

not interconvertible, since thermolysis of **C** gives **A**, **B**, and $(\mu\text{-H})Os_3(CO)_9(\mu_3,\eta^3\text{-}$ $(CPh)_3)$, but no **D** is formed; similar results are observed by heating **D**. Comparably, the two isomers of $Os_3(CO)_8(H(CPh)_5)$, **A** and **B**, are not converted to each other upon heating. However, in the presence of CO, isomerization of **A** to **B** (and vice versa) does occur, apparently via $Os_3(CO)_9(H(CPh)_5)$. Treatment of $Os_3(CO)_8(H(CPh)_5)$ with CO generates $Os_3(CO)_9(H(CPh)_5)$. Since **A** and **B** react with CO to give mainly **D** and **C**, respectively, this suggests that the pairs **A**, **D** and **B**, **C** may be most closely related.

*The crystal and molecular structure of **B**, now shown to be $Os_3(CO)_8(\mu,\eta^2\text{-}$ $CPhCHPh)(\mu,\eta^3\text{-}C_3Ph_3)$*

The crystal contains discrete molecular units, separated by normal Van der Waals' distances; there are no abnormally short intermolecular contacts. The molecular geometry and atomic labelling are depicted in Fig. 1. The molecule is chiral (C_1 symmetry) but the crystal contains an ordered array of the two enantiomeric forms by virtue of the crystallographic operations (viz., 1 and 2_1 and $\bar{1}$ and c for space group $P2_1/c$). A stereoscopic view of the molecule appears as Fig. 2; interatomic distances and angles are compiled in Tables 3 and 4.

The molecule is hereby identified as $Os_3(CO)_8(\mu\text{-}\eta^2\text{-}CPhCHPh)(\mu,\eta^3\text{-}C_3Ph_3)$. The molecule is formally derived from $Os_3(CO)_{12}$ by replacing four terminal CO ligands by a three-electron donating $\mu\text{-}\eta^2\text{-}CHPh=CPh$ ligand (a σ, π-vinyl system) and a five-electron donating $\mu\text{-}\eta^3\text{-}C_3Ph_3$ ligand (yielding a dimetalla-allyl fragment). The Os–Os distances show substantial variation. Compared to $Os_3(CO)_{12}$, in which Os–Os(av.) = 2.877(3) Å [7], we find the bridged Os–Os bonds to be shortened (Os(1)–Os(2) = 2.764(2) and Os(1)–Os(3) = 2.694(2) Å) and the non-bridged bond to be lengthened (Os(2)–Os(3) = 3.015(2) Å); the average Os–Os distance is now 2.824 Å. The average Os–CO distance is 1.810 ± 0.12 Å with C–O 1.20 ± 0.06 Å; all Os–C–O systems are close to linear (169.6–177.7°). The rather poor quality of the diffraction data appears to affect particularly the locations of the carbon atoms in the carbonyl groups; the organic ligands show far less deviation from accepted values.

The μ,η^2-vinyl ligand is σ-bonded to Os(1) (Os(1)–C(7) = 2.184(30) Å) and π-bonded to Os(3) (Os(3)–C(7) = 2.260(30) Å, Os(3)–C(8) = 2.276(28) Å); the coor-
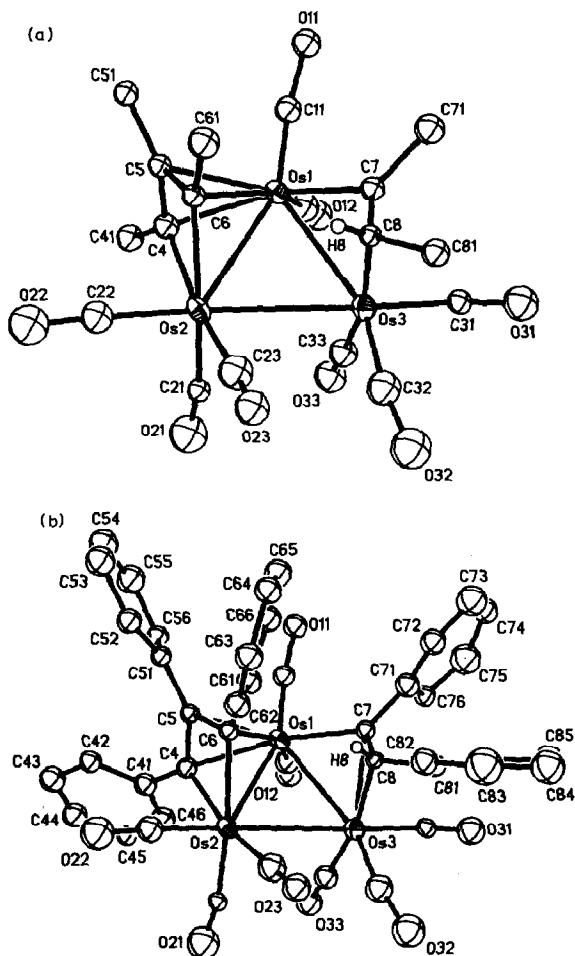
Fig. 1. Molecular geometry and atomic labelling for $Os_3(CO)_8(\mu,\eta^2\text{-CPhCHPh})(\mu,\eta^3\text{-C}_3Ph_3)$ (**B**). (a) The molecular core (note that the Os(3)–C(7) linkage is hidden from view); (b) all non-hydrogen atoms (note here that the Os(1)–C(5) linkage is almost hidden from view). These are both ORTEP-II diagrams, with ellipsoids drawn at the 50% probability level.

dinated $C(7)=C(8)$ distance is 1.38(4) Å. The $\mu,\eta^3\text{-C}_3Ph_3$ fragment is π-bonded to Os(2) (Os(2)–C(6) = 2.120(30) Å compared to Os(2) $\cdots$ C(5) = 2.723(31) Å) and is bonded in an η^3-fashion to Os(1) (Os(1)–C(4) = 2.206(32) Å, Os(1)–C(5) = 2.258(33) Å, Os(1)–C(6) = 2.276(21) Å); carbon–carbon distances within the η^3-allyl system are C(4)–C(5) = 1.42(5) and C(5)–C(6) = 1.47(4) Å (av. 1.445 Å).

Distances within the organic ligand are internally consistent and well behaved with C–Ph = 1.45(5)–1.55(4) Å (average = 1.50 ± 0.04 Å) and C–C(phenyl) = 1.29(6)–1.49(6) Å (average = 1.396 ± 0.048 Å).

Spectroscopic characterization of compounds A and B

Both **A** and **B** isomers of $Os_3(CO)_8(H(CPh)_5)$ have been characterized by spectroscopic methods, but we have not been able to obtain crystals of **A** suitable for X-ray diffraction studies. The close resemblance of their IR ($\nu(CO)$) spectra, shown in Fig. 3, suggests that their structures also should be closely similar,
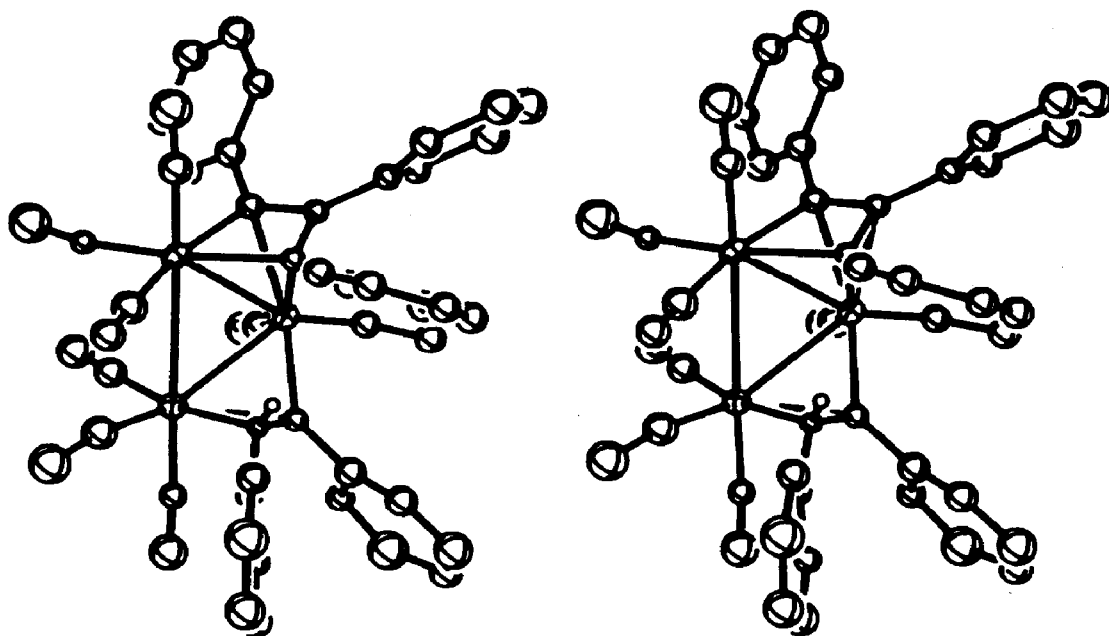
Fig. 2. A stereoscopic view of $Os_3(CO)_8(\mu,\eta^2\text{-CPhCHPh})(\mu,\eta^3\text{-C}_3Ph_3)$ (B).

Table 3

Interatomic distances (Å), with Esd's, for $Os_3(CO)_8(\mu,\eta^2\text{-CPhCHPh})(\mu,\eta^3\text{-C}_3Ph_3)$ (B)

Osmium – osmium distances			
Os(1)–Os(2)	2.764(2)	Os(2)–Os(3)	3.015(2)
Os(1)–Os(3)	2.694(2)		
Osmium – carbon (bridging ligand) distances			
Os(1)–C(4)	2.206(32)	Os(1)–C(5)	2.258(33)
Os(1)–C(6)	2.276(31)	Os(1)–C(7)	2.184(30)
		Os(1) ⋯ C(8)	3.048(27)
Os(2)–C(4)	2.151(31)	Os(2) ⋯ C(5)	2.723(31)
Os(2)–C(6)	2.120(30)	Os(3)–C(7)	2.260(30)
Os(3)–C(8)	2.276(28)		
Selected distances within the organic ligands			
C(4)–C(5)	1.42(5)	C(5)–C(51)	1.47(5)
C(5)–C(6)	1.47(4)	C(6)–C(61)	1.51(4)
C(7)–C(8)	1.38(4)	C(7)–C(71)	1.45(5)
C(4)–C(41)	1.52(5)	C(8)–C(81)	1.55(4)
Osmium – carbonyl and carbon – oxygen distances			
Os(1)–C(11)	1.60(3)	C(11)–O(11)	1.32(4)
Os(1)–C(12)	1.89(4)	C(12)–O(12)	1.15(5)
Os(2)–C(21)	1.86(3)	C(21)–O(21)	1.16(4)
Os(2)–C(22)	1.85(4)	C(22)–O(22)	1.18(5)
Os(2)–C(23)	1.91(4)	C(23)–O(23)	1.19(4)
Os(3)–C(31)	1.83(4)	C(31)–O(31)	1.20(5)
Os(3)–C(32)	1.66(4)	C(32)–O(32)	1.28(5)
Os(3)–C(33)	1.89(4)	C(33)–O(33)	1.15(5)

Table 4

Interatomic angles ($^\circ$) with esd's for $Os_3(CO)_8(\mu,\eta^2\text{-CPhCHPh})(\mu,\eta^3\text{-}C_3Ph_3)$ (**B**)

Intermetallic angles			
Os(1)–Os(2)–Os(3)	55.4(1)	Os(2)–Os(1)–Os(3)	67.1(1)
Os(2)–Os(3)–Os(1)	57.6(1)		
Os–Os–CO angles			
Os(2)–Os(1)–C(11)	154.0(12)	Os(2)–Os(1)–C(12)	114.3(12)
Os(3)–Os(1)–C(11)	136.3(12)	Os(3)–Os(1)–C(12)	86.7(12)
Os(1)–Os(2)–C(21)	115.3(10)	Os(1)–Os(2)–C(22)	130.2(12)
Os(1)–Os(2)–C(23)	120.4(12)	Os(3)–Os(2)–C(21)	87.2(11)
Os(3)–Os(2)–C(22)	169.7(12)	Os(3)–Os(2)–C(23)	76.2(12)
Os(1)–Os(3)–C(31)	119.6(12)	Os(1)–Os(3)–C(32)	150.2(12)
Os(1)–Os(3)–C(33)	95.9(12)	Os(2)–Os(3)–C(31)	176.8(12)
Os(2)–Os(3)–C(32)	95.0(12)	Os(2)–Os(3)–C(33)	87.9(12)
Os–C–O and C–Os–O angles			
Os(1)–C(11)–O(11)	172.3(28)	C(11)–Os(1)–C(12)	82.5(17)
Os(1)–C(12)–O(12)	176.4(33)	C(21)–Os(2)–C(22)	96.4(15)
Os(2)–C(21)–O(21)	169.6(29)	C(21)–Os(2)–C(23)	92.3(15)
Os(2)–C(22)–O(22)	175.2(33)	C(22)–Os(2)–C(23)	93.9(17)
Os(2)–C(23)–O(23)	168.9(32)	C(31)–Os(3)–C(32)	88.1(17)
Os(3)–C(31)–O(31)	175.4(29)	C(31)–Os(3)–C(33)	90.9(15)
Os(3)–C(32)–O(32)	169.9(34)	C(32)–Os(3)–C(33)	94.4(18)
Os(3)–C(33)–O(33)	177.7(32)		
Angles involving the bridging ligands			
Os(2)–Os(1)–C(4)	49.8(8)	Os(3)–Os(1)–C(4)	111.1(8)
Os(1)–Os(2)–C(4)	51.5(9)	Os(3)–Os(2)–C(4)	102.0(8)
C(7)–Os(1)–C(4)	145.7(12)	Os(1)–C(4)–Os(2)	78.7(11)
Os(1)–C(4)–C(41)	132.2(23)	Os(1)–C(4)–C(5)	73.5(18)
Os(2)–C(4)–C(41)	127.5(23)	Os(2)–C(4)–C(5)	97.3(21)
C(41)–C(4)–C(5)	128.7(29)	Os(2)–Os(1)–C(5)	64.8(8)
Os(3)–Os(1)–C(5)	130.6(8)	C(7)–Os(1)–C(5)	124.4(11)
Os(1)–C(5)–C(4)	69.5(18)	Os(1)–C(5)–C(51)	123.5(21)
Os(1)–C(5)–C(6)	71.8(17)	C(4)–C(5)–C(51)	128.6(28)
C(4)–C(5)–C(6)	101.2(26)	C(51)–C(5)–C(6)	130.1(27)
Os(2)–Os(1)–C(6)	48.6(8)	Os(3)–Os(1)–C(6)	99.1(8)
Os(1)–Os(2)–C(6)	53.6(8)	Os(3)–Os(2)–C(6)	93.6(8)
C(7)–Os(1)–C(6)	90.2(11)	Os(1)–C(6)–Os(2)	77.8(10)
Os(1)–C(6)–C(5)	70.4(17)	Os(1)–C(6)–C(61)	120.3(21)
Os(2)–C(6)–C(5)	97.0(19)	Os(2)–C(6)–C(61)	141.3(23)
C(5)–C(6)–C(61)	120.7(27)	Os(2)–Os(1)–C(7)	98.8(8)
Os(3)–Os(1)–C(7)	54.0(8)	Os(2)–Os(3)–C(7)	90.2(8)
Os(1)–C(7)–Os(3)	74.6(10)	Os(1)–C(7)–C(71)	120.3(23)
Os(1)–C(7)–C(8)	115.9(21)	Os(3)–C(7)–C(71)	132.9(23)
C(71)–C(7)–C(8)	122.5(29)	Os(1)–Os(3)–C(8)	75.1(7)
Os(2)–Os(3)–C(8)	83.0(7)	Os(3)–C(7)–C(8)	73.0(17)
Os(3)–C(8)–C(7)	71.7(17)	Os(3)–C(8)–C(81)	121.3(19)
C(81)–C(8)–C(7)	130.6(27)		

probably differing only in the relative positioning of the $\mu\text{-}C_3Ph_3$ and the $\mu\text{-}C_2Ph_2H$ groups around the triosmium framework. The ^1H NMR spectrum of $Os_3(CO)_8(H(CPh)_5)$ (**B**) shows a multiplet between δ 7.45 and 6.67(25H) for the phenyl protons and a 1H singlet at δ 6.29 for the proton attached to the substituted vinyl group. The analogous vinylic proton resonances are at δ 6.99 in
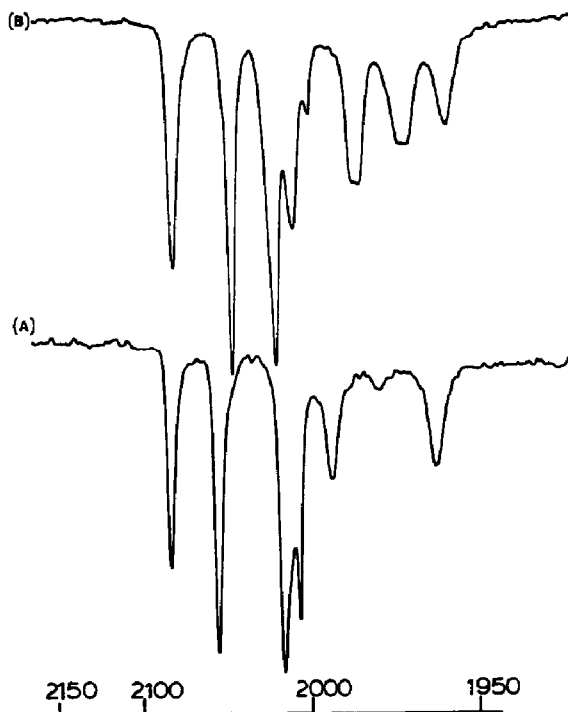
Fig. 3. IR spectra in the carbonyl region of $Os_3(CO)_8(H(CPh)_5)$ (A) and $Os_3(CO)_8(H(CPh)_5)$ (B), shown to be $Os_3(CO)_8(\mu,\eta^2\text{-CPhCHPh})(\mu,\eta^3\text{-}C_3Ph_3)$; obtained in cyclohexane.

$HOs_3(CO)_{10}(\mu,\eta^2\text{-CPh=CHPh})$ [8] and at δ 5.91 in $CpWOs_3(CO)_7(\mu\text{-O})(\mu\text{-}H)_2(\mu_4,\eta^2\text{-CCHTol})(\mu,\eta^2\text{-CPh=CHPh})$ [9]. The ^1H NMR spectrum of $Os_3(CO)_8(H(CPh)_5)$ (A) shows the phenyl proton multiplet in the range δ 7.31–6.19 together with a singlet at δ 5.11 (1H), which is assigned to a vinylic proton.

The ^{13}C NMR spectra of $Os_3(^*CO)_8(H(CPh)_4{}^*CPh)$ (A) and (B) are illustrated in Fig. 4. The spectrum of A shows eight 1C signals in the range δ 186.8–174.1 for the carbonyl carbons and two 0.5C resonances at δ 155.2 and 130.5 for the C-Ph carbons. Correspondingly, the spectrum of B shows eight 1C resonances between δ 187.0–172.7 and two 0.5C signals at δ 121.4 and 109.8. Splitting of the ^{13}C enriched $^*C$-Ph carbon into two 0.5C signals for B implies that the two ends of the linked C_3Ph_3 unit became equivalent, probably during its formation. The similar result for A again implies an analogous structure. Note that the bonding characters of C(4) and C(6) in the structure of B are not very different (see Fig. 1) and that they could be interchanged by C(4) moving below the Os_3 plane while C(6) moves into this plane. However, this interchange of positions would not truly equilibrate C(4) and C(6), since the hydrogen position at C(8) makes the two faces of the Os_3 plane inequivalent. Complete equilibration, therefore, would require inversion of configuration at C(8). This could be done through a σ,π-interchange process [8], but further extensive rearrangement would be necessary for complete equilibration.

Spectroscopic characterization of compounds C and D

The two isomers of $Os_3(CO)_9(H(CPh)_5)$, C and D, have been characterized spectroscopically. The IR absorption patterns for both isomers, shown in Fig. 5, are very similar. The presence of low wavenumber peaks for C (1923 cm^{-1}) and D
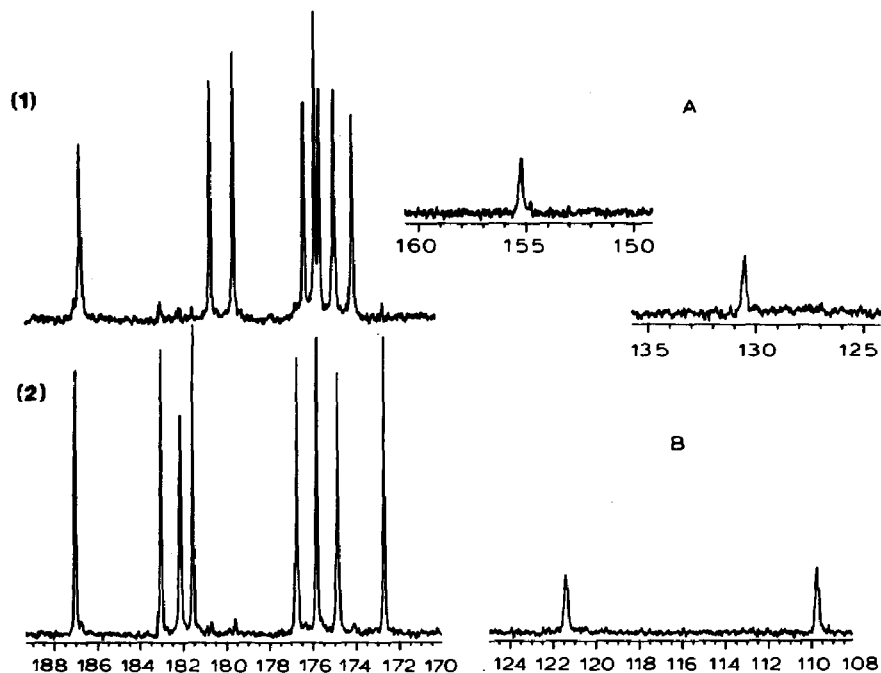
(1)

(2)

A

B

Fig. 4. 90 MHz ^{13}C NMR spectra of (1) $Os_3(*CO)_8(H(CPh)_4*CPh))$ (A) and (2) $Os_3(*CO)_8(H(CPh)_4-*CPh)$ (B); obtained in $CDCl_3$ at $-55\,^{\circ}C$.

$(1966\ cm^{-1})$ suggests in each case a bridging carbonyl ligand, although these are rather rare for triosmium compounds [10,11].

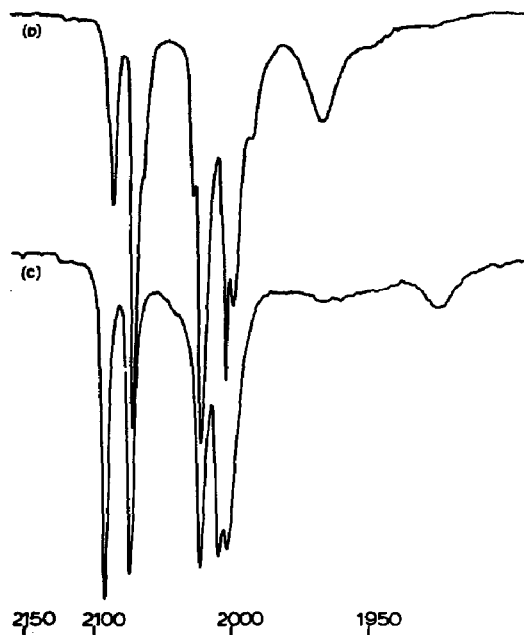In the ^{1}H NMR spectrum of **C**, the phenyl protons appear as a complex multiplet

Fig. 5. IR spectra in the carbonyl region of $Os_3(CO)_9(H(CPh_5))$ (C) and $Os_3(CO)_9(H(CPh)_5)$ (D); obtained in cyclohexane.

between δ 7.32 and 6.64 (25H), with the proton bound to one of the C-Ph groups appearing as a singlet at δ 5.05 (1H). Similarly, the ^{1}H NMR spectrum of **D** shows a multiplet in the range δ 7.57–6.74 (25H) and a singlet at δ 4.42 (1H), which are assigned analogously.

The ^{13}NMR spectrum of $Os_3(^*CO)_9(H(CPh)_4{}^*CPh)$ (**C**) shows a 1C resonance at δ 218.8 assignable to a bridging carbonyl, eight 1C signals in the range δ 187.4–171.6 corresponding to the remaining carbonyls, and a 1C signal at δ 1.48 for a *C*-Ph carbon. The ^{13}C NMR spectrum of $Os_3(^*CO)_9(H(CPh)_4{}^*CPh)$ (**D**) shows a signal at δ 203.3, which is attributed to a bridging carbonyl, together with eight 1C resonances between δ 183.0 and 170.5, which are assigned to the terminal carbonyl carbons. Finally, the two 0.5 C resonances at δ 129.2 and 90.0 are assigned to two *C*-Ph carbons.

Although the structures of **C** and **D** are not known in detail, it seems very unlikely, in view of the observed interconversions with compounds **A** and **B**, that the basic carbon–carbon connectivities differ significantly. Therefore, **C** and **D** both presumably contain a separate C_3Ph_3 unit and a vinylic C_2Ph_2H unit. This is entirely consistent with the spectroscopic data, although we cannot eliminate the alternative of a CPhCPhCHPh unit and a complexed diphenylacetylene. In either case one of the ligands would have to donate two electrons less in order to accommodate the added carbonyl, or a metal–metal bond could be broken. The simplest change, in comparison with the structure of **B** shown in Fig. 1, would be the decomplexation of C(5) and C(6) from Os(1), thereby converting the dimetalla–allyl moiety from $\pi(\eta^3)$ to $\sigma(\eta^1)$ bonding at Os(1).

Spectroscopic characterization of $(\mu$-H)Os$_3$(CO)$_9(\mu_3,\eta^3$-CPh)$_3$)

The IR and ^{1}H NMR spectra of $(\mu$-H)Os$_3$(CO)$_9(\mu_3,\eta^3$-(CPh)$_3$) are in close agreement with those of $(\mu$-H)Os$_3$(CO)$_9(\mu_3,\mu^3$-(CPh)$_2$COMe) [12] $(\mu$-H)Os$_3$(CO)$_9$-$(\mu_3,\eta^3$-CHC$_6$H$_4$) [1], $(\mu$-H)Os$_3$(CO)$_9(\mu_3,\eta^3$-(CPh)$_2$CH) [13] and $(\mu$-H)Os$_3$(CO)$_9$-$(\mu_3,\eta^3$-(CH)$_2$COMe) [14] each of which has a face-bonded dimetallaallyl ligand. The ^{1}H NMR spectrum of $(\mu$-H)Os$_3$(CO)$_9(\mu_3,\eta^3$-(CPh)$_3$ shows the phenyl protons as a
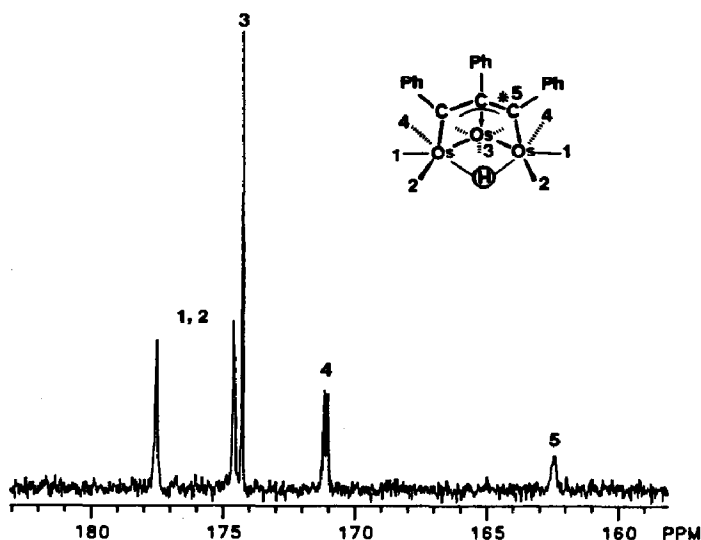
Fig. 6. 90 MHz ^{13}C NMR spectrum of $(\mu$-H)Os$_3(^*CO)_9(\mu_3,\eta^2$-(CPh)$_2{}^*$CPh) in CDCl$_3$ at 17°C.

complex multiplet in the range δ 7.10–6.66 (15H), and a singlet at δ −18.16 (1H) for the bridging hydride.

The ^{13}C NMR spectrum of $(\mu\text{-H})Os_3(^{\star}CO)_9(\mu_3,\eta^3\text{-}(CPh)_2{}^{\star}CPh)$ generated from $(\mu\text{-H})Os_3(^{\star}CO)_{10}(\mu_3\text{-}^{\star}CPh)$ (ca. 50% ^{13}C enriched) is shown in Fig. 6. The carbonyl carbons are in a 2/2/3/2 pattern, which agrees with the proposed symmetric structure. The 2C signals at δ 177.5 and 174.6 are assigned to two pairs of carbonyls bound to the hydride-bridged osmium atoms. The 3C signal at δ 174.2 is assigned to the three carbonyls in the $Os(CO)_3$ unit facing the bridging hydride, presumably undergoing equilibration via three fold rotation. The 2C signal at δ 171.1 appears as a doublet ($^2J(\text{C--H})$ 11 Hz) and is assigned to the two carbonyls located *trans* to the hydride. The signal at δ 162.4 is appropriate for an α carbon of the metallated allyl group, since a more upfield position would be expected for the β-carbon [12].

Conclusion

Keister and coworkers [12] have conducted extensive studies of alkylidyne-alkyne coupling with alkylidyne triruthenium complexes. In particular either $(\mu\text{-}H)Ru_3(CO)_{10}(\mu\text{-COMe})$ or $(\mu\text{-H})_3Ru_3(CO)_9(\mu_3\text{-COMe})$ reacts with diphenyl-acetylene to give $(\mu\text{-H})Ru_3(CO)_9(\mu^3,\eta^3\text{-C(OMe)CPhCPh})$; similarly, $(\mu\text{-H})_3\text{-}Ru_3(CO)_9(\mu_3\text{-CPh})$ gives $(\mu\text{-H})Ru_3(CO)_9(\mu_3,\eta^3\text{-CPhCPhCPh})$ and $(\mu\text{-H})Os_3\text{-}(CO)_{10}(\mu\text{-COMe})$ gives $(\mu\text{-H})Os_3(CO)_9(\mu^3,\eta^3\text{-C(OMe)CPhCPh})$. Thus, we expected the reaction of $(\mu\text{-H})Os_3(CO)_{10}(\mu\text{-CPh})$ with diphenylacetylene to give $(\mu\text{-H})Os_3\text{-}(CO)_9(\mu_3,\eta^3\text{-CPhCPhCPh})$. Indeed, this reaction is observed, but it is accompanied by a significant amount of reaction with a second equivalent of the alkyne to give both nonacarbonyl and octacarbonyl products. The crystal structure of compound **B**, an octacarbonyl product, shows that one molecule of the alkyne has indeed coupled to the initial benzylidyne moiety, giving a C_3Ph_3 unit, but that the second molecule has inserted into the metal hydride linkage to give a vinylic C_2Ph_2H unit. On the basis of spectroscopic data, we argue that **A** has a structure very similar to that of **B**, essentially a geometric isomer. Likewise, we conclude that **C** and **D**, the nonacarbonyl products, have the same basic hydrocarbyl units. However, the exact effect of the added carbonyl ligand, other than to induce one bridging carbonyl, cannot be determined. Both **C** and **D** give traces of $(\mu\text{-H})Os_3(CO)_9(\mu_3,\eta^3\text{-}C_3Ph_3)$ upon pyrolysis, implying that the inserted alkyne can be eliminated from the vinylic group. However, the low yield of this reaction and the fact that it cannot be reversed indicate that under preparative conditions the formation of **C** and **D** is not linked with the formation of $(\mu\text{-H})Os_3(CO)_9(\mu_3,\eta^3\text{-}C_3Ph_3)$. Given the relative yields from the reaction, it is likely that compounds **A** and **B** are the other primary products. Under the reaction conditions, these apparently trap carbon monoxide from solution to give compounds **C** and **D**.

Supplementary material available

A list of observed and calculated structure factor amplitudes in available upon request from one of us (M.R.C.).

References

1 W.-Y. Yeh, J.R. Shapley, Y.-J. Li and M.R. Churchill, Organometallics, 4 (1985) 767.
2 M.R. Churchill, R.A. Lashewycz and F.J. Rotella, Inorg. Chem., 16 (1977) 265.

3 International Tables for X-Ray Crystallography, Vol. 1, Kynoch Press, Birmingham, England, 1965, p. 99.
4 International Tables for X-Ray Crystallography, Vol. 4, Kynoch Press, Birmingham, England (1974): (a) pp. 99–101; (b) pp. 149–150.
5 G. Germain, P. Main and M.M. Woolfson, Acta Cryst., A27 (1971) 368.
6 M.R. Churchill, Inorg. Chem., 12 (1973) 1213.
7 M.R. Churchill and B.G. DeBoer, Inorg. Chem., 16 (1977) 878.
8 A.D. Clauss, M. Tachikawa, J.R. Shapley and C.G. Pierpont, Inorg. Chem., 20 (1981) 1528.
9 (a) Y. Chi, J.R. Shapley, M.R. Churchill and J.W. Ziller, unpublished results; (b) Y. Chi, Ph.D. Thesis, University of Illinois at Urbana-Champaign, 1986.
10 G.R. Steinmetz and G.L. Geoffroy, J. Am. Chem. Soc., 103 (1981) 1278.
11 J.R. Shapley, A.C. Sievert, M.R. Churchill and H.J. Wasserman, J. Am. Chem. Soc., 103 (1981) 6975.
12 L.R. Beanan and J.B. Keister, Organometallics, 4 (1985) 1713.
13 A.D. Clauss, J.R. Shapley and S.R. Wilson, J. Am. Chem. Soc., 103 (1981) 7387.
14 B.E. Hanson, B.F.G. Johnson, J. Lewis and P.R. Raithby, J. Chem. Soc., Dalton Trans., (1980) 1852.